Hindawi
Journal of Food Biochemistry
Volume 2023, Article ID 6615768, 15 pages
https://doi.org/10.1155/2023/6615768

Research Article

Network Pharmacology-Based Approach to Explore the Total Flavonoids of *Phellinus igniarius* against Hyperuricemia via Regulating the Nrf2/HO-1-ROS-ER Signaling Pathway

Mengling Lv, Zhouqin Liu, Yuling Tao, Chenlei Jiang, and Hong Lu

School of Pharmaceutical Sciences, Zhejiang Chinese Medical University, Hangzhou, China

Correspondence should be addressed to Hong Lu; luhong@zcmu.edu.cn

Received 6 July 2023; Revised 25 September 2023; Accepted 14 October 2023; Published 2 November 2023

Academic Editor: Adadi Parise

Based on the antioxidant properties of *Phellinus igniarius* (DC. Ex Fr.) Quel (*P. igniarius*), this study aims to investigate the protective effect and mechanism of total flavonoids of *Phellinus igniarius* (TFPI) on the oxidative damage of HK-2 cells induced by monosodium urate (MSU). The GO and KEGG enrichment analyses predicted the potential targets and pathways of TFPI in the treatment of hyperuricaemia (HUA). We used MSU to stimulate HK-2 cells to establish a HUA model. Cell viability, lactate dehydrogenase (LDH) assay, and reactive oxygen species (ROS) assay were performed. Cell nuclear morphology was detected with DAPI and Annexin V-FITC. The activity of superoxide dismutase (SOD) and malondialdehyde (MDA) was analyzed. The expression of Keap 1, Nrf2, HO-1, Bip, PERK, ATF4, CHOP, BAX, Bcl-2, and cleaved caspase 3 was performed with western blot. The results of network pharmacology showed that the potential targets and pathways were mainly associated with stimulus response, regulation of reactive oxygen species metabolic processes, response to oxidative stress, and regulation of the response to the endoplasmic reticulum (ER) stress pathway. The cell experiment proved that the survival rate of HK-2 cells was dramatically increased after treatment with TFPI. TFPI increased the activity of SOD and decreased the content of MDA and LDH, while scavenging ROS. TFPI increased the transfer of Nrf2 protein from the cytoplasm to the nucleus and decreased the expression level of Bip, PERK, ATF4, CHOP, BAX, and cleaved caspase 3 to attenuate apoptotic cells induced by MSU. TFPI has a good protective effect on MSU-induced oxidative damage in HK-2 cells and can reduce cell apoptosis by regulating ROS-mediated ER stress.

1. Introduction

Hyperuricemia (HUA) is a metabolic disorder caused by abnormal purine metabolism or reduced uric acid excretion with elevated blood uric acid (UA) as the main feature [1]. Studies have shown that chronically high UA levels cause kidney damage by depositing excess UA in the renal tubules in patients with HUA [2]. Emerging data demonstrated that UA was closely associated with illnesses related to acute kidney injury, chronic kidney disease, and cardiovascular disease [3, 4]. As the end products of purine metabolism in higher primates, UA triggers the production of free radicals and oxidative stress in several cells [5–7]. Excessive accumulation of UA leads to an increase in oxygen radicals and reactive oxygen species (ROS), causing crystal deposits in the renal tubules. This process induces oxidative stress which can trigger mechanical damage or inflammatory responses in the body and ultimately result in impaired renal function [8, 9]. Oxidative stress might be involved as pathogenic factors in the development of early HUA and related renal diseases, but specific mechanisms are still to be elucidated.

Phellinus igniarius (DC. Ex Fr.) Quel (*P. igniarius*) belongs to the family Polyporaceae, which is a kind of a precious medicinal and edible fungus with good antioxidant and hepatorenal protection [10]. HUA was known as "arthralgia syndrome" in Chinese medicine, and *P. igniarius* was recorded in the "Xinxiu Ben Cao" served as a treatment for arthralgia syndrome in the Tang Dynasty (618–907 AD) [11]. Recent studies have indicated that *P. igniarius* extract could affect the expression of xanthine oxidase (XO) to effectively reduce the serum UA level of HUA mice and improve the degree of uric acid renal pathological injury

[12, 13]. Our previous study found that *P. igniarius* could not only inhibit ROS production but also promote the expression of ABCG2 by targeting the TLR4 receptor and the NLRP3 inflammasome in the MSU-induced HK-2 cells [14]. Moreover, ethanol extracts of *P. igniarius* have been reported to have a good renal protective effect against oteracil potassium-induced injury and could also regulate the gut microbiota to reduce blood UA levels [15]. Research on polysaccharides, flavonoids, polyphenols, and other active ingredients from *P. igniarius* [16] have been reported on antitumor [17, 18], antiinflammatory [19], antioxidative [20], and enhancing immunity [21]. Based on the antioxidant potential of *P. igniarius* and previous research foundations, this article will continue to use the MSU-induced HK-2 cell injury model as the research object. The antioxidant N-acetyl-L-cysteine (NAC) group was added to further explore the protective effect and mechanism of total flavonoids of *Phellinus igniarius* (TFPI) on MSU-induced oxidative damage in HK-2 cells.

Network pharmacology describes the complex pharmacological mechanism of traditional Chinese medicine (TCM) with multicomponents and multitargets from the perspective of a network and reveals the overall analysis strategy of the mechanism of TCM treatment of diseases [22, 23]. Network pharmacology is increasingly being used to explore the pharmacological mechanisms of medicinal plants and raw drugs [24].

Therefore, we investigated the effect and mechanism of TFPI on MSU-induced oxidative damage in HK-2 cells by combining network pharmacology. The flowchart of the research performed in this study is shown in Figure 1.

2. Materials and Methods

2.1. Network Pharmacology

2.1.1. Chemical Ingredients of P. igniarius. The chemical ingredients of *P. igniarius* were obtained from (1) Traditional Chinese Medicine Systems Pharmacology Database and Analysis Platform (TCMSP, https://tcmspw.com/tcmsp.php, version 2.3) and (2) Traditional Chinese Medicines Integrated Database (TCMID, https://www.megabionet.org/tcmid/). In meantime, we also manually retrieved the ingredients from published literature. In order to identify the compounds that may improve HUA, the SwissTargetPrediction tool was used, which described the absorption, distribution, metabolism, and elimination (ADME) system. The information of these ingredients was presented at the SwissADME (https://www.swissadme.ch/). The screening criteria for ingredient mainly include OB ≥ 30%; DL ≥ 0.18; GI absorption is "High." and Lipinski information.

2.1.2. Target Prediction. First, all the screened ingredients were added to PubChem (https://pubchem.ncbi.nlm.nih.gov/) to capture the Canonical SMILES. Second, each SMILES was imported into the Swiss Target Prediction (https://www.swisstargetprediction.ch/) and SEA Target System (https://sea.bkslab.org/) to predict the potential target genes related to multiple diseases in human. Third, HUA-related genes were obtained from the DisGeNET database (https://www.disgenet.org/), which mostly contained the largest number of genes associated with human diseases. Lastly, the overlapping genes of HUA and the ingredient of *P. igniarius* were collected, which are potential target genes of *P. igniarius* for the treatment of HUA. Then, an "ingredients–target" network was constructed in the Cytoscape 3.7.2 software.

2.1.3. Functional Enrichment of P. igniarius's Therapeutic Targets for HUA. The related target genes were imported into the Metascape system for TRRUST enrichment analysis. During this analysis, terms with $P < 0.01$, minimum count of 3, and the enrichment factor >1.5 were settled. The gene ontology (GO) functions of the target genes and the Kyoto Encyclopedia of Genes and Genomes (KEGG) pathways were also annotated by R and RStudio software. Finally, the first 20 enrichment analysis results were visualized.

2.2. Pharmacodynamic Experiment

2.2.1. Preparation of TFPI. The dried fruit entities of *P. igniarius* (20180716, Zhejiang Qian Dao Lake Sangdu Edible Fungus Professional Cooperative, China) were crushed and sieved. After soaking in 70% ethanol for 0.5 h, the powder was refluxed for 1 h and then purified by filtration. The filter residue was washed with 70% ethanol. The filtrates were combined and placed in a rotary evaporator to recover the ethanol until there was no alcoholic smell, and then the crude ethanol extract of *P. igniarius* was obtained. The crude extract was wet loaded in an activated AB-8 microporous adsorbent resin, left for 1 h, and eluted with 70% ethanol. The collected ethanol eluate was concentrated and then freeze-dried to obtain the purified TFPI. The total flavonoids were 66.7%, as measured by the rutin-AlCl3 method [14, 25]. The test drug was filtered by a 0.22 μm filter membrane and sterilized, then stored at −20°C until further required.

2.2.2. Cell Culture and Treatments. The HK-2 cell line was obtained from ATCC and maintained in DMEM/F12. Monosodium urate (MSU) crystal-induced HK-2 cells were a cell model for HUA. To investigate the protective effect of TFPI on MSU-induced oxidative damage in HK-2 cells, HK-2 cells were treated with MSU (150 μg/mL, sigma), MSU + TFPI (37.5, 75, 150 μg/mL), and N-acetyl-L-cysteine (NAC, 1 mmol/L) for 24 h.

2.2.3. Cell Viability Assays. HK-2 cells were divided into control, model (150 μg/mL MSU), MSU (150 μg/mL) + TFPI (37.5, 75, 150 μg/mL), and NAC (1 mmol/L) groups with inoculation into 96-well plates incubated in a constant temperature incubator for 24 h. After different treatment regimens, 20 μL of MTT agent (5 mg/mL) was added and incubated for 4 h with light protection. After that, 150 μL of DMSO per well was added, protected from light, and shaken

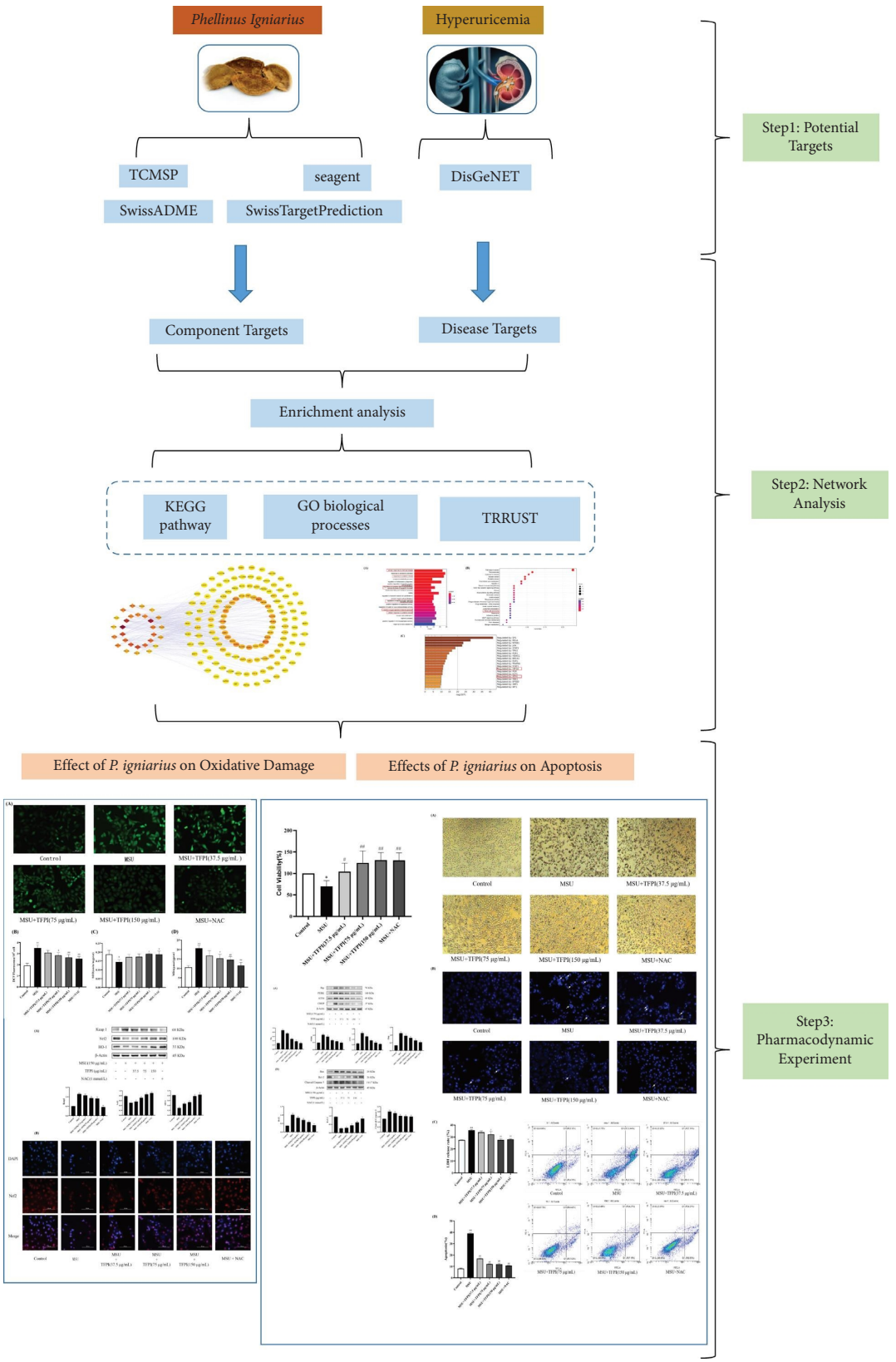

Figure 1: The schematic diagram of the present study.

for 10 min to solubilize the blue-purple crystals. The absorbance of each well was measured at 490 nm using the enzyme marker.

2.2.4. Lactate Dehydrogenase (LDH) Assay. When HK-2 cells (1×10^5 mL^{-1}) were grown to 70%–80% in 6-well plates, they were then treated for 24 h with different treatment regimens according to 2.2.2. The levels of LDH released from plasma membrane ruptured cells were detected using commercial detection kits (E1020, Puli Gene Technology Co. Ltd., China) following the assay instructions. The absorbance was measured at 440 nm on an enzyme-standard instrument.

2.2.5. Cell Nuclear Morphology Detection. Nuclear apoptosis was detected by 4-6-diamidino-2-phenylindole (DAPI, D9542-1MG, Sigma, USA) staining. Briefly, different groups of cells (1×10^5 mL^{-1}) treated according to 2.2.2 were stationary in 4% paraformaldehyde for 10 min, washed with PBS, and stained with DAPI (0.2 μg/mL) for 20 min, protected from light, and visualized with a fluorescence-inverted microscope.

2.2.6. ROS Assay. Intracellular superoxide production was observed with 2,7-dichlorodi-hydrofluorescein diacetate (DCF-DA) (S0033-1, Beyotime Bioengineering Institute). HK-2 cells (1×10^5 mL^{-1}) were inoculated into 6-well plates, grouped according to 2.2.2, and treated for 24 h. The cells were incubated in serum-free medium with DCFH-DA staining solution (10 μM/L) for 20 min under light-proof conditions, and visualized with a fluorescence-inverted microscope.

2.2.7. Detection of Malondialdehyde (MDA) and Superoxide Dismutase (SOD). HK-2 cells (1×10^5 mL^{-1}) were seeded in 6-well plates and treated for 24 h according to 2.2.2. The levels of lipid oxidation as well as superoxide dismutase were detected by the MDA kit (S0131, Bioengineering Institute of Bain Marie, China) and the SOD kit (S0101S, Bioengineering Institute of Bain Marie, China), respectively.

2.2.8. Annexin V-FITC Apoptosis Detection Kit. HK-2 cells (1×10^5 mL^{-1}) were seeded in 6-well plates and treated for 24 h according to 2.2.2. The apoptosis rate was detected by the Annexin V-FITC apoptosis detection kit (C1062L, Beyotime Bioengineering Institute).

2.2.9. Western Blot Analysis. On the basis of western blotting, we investigated the expression of oxidative stress, apoptosis, and ER-associated proteins. After fixing the concentration, loading the sample, and wet transferring the membrane, polyvinylidene difluoride (PVDF) membranes were incubated with specific primary antibodies at 4°C overnight. After washing with TBST buffer, the membranes were incubated with secondary antibodies at room temperature for 2 hours. Analysis was performed with ImageJ System software after visualization using an enhanced chemiluminescence kit (190–5070, Bio-Rad, USA).

2.2.10. Immunofluorescence (IF). The prepared HK-2 cells were first fixed with 4% paraformaldehyde for 15 min and then permeabilized with 0.5% Triton X-100 for 1 h. Then the cells were sealed for 1 h, and the primary antibody (according to antibody instructions: Nrf2 at a dilution of 1 : 100) was added with shaking at 4°C overnight. After washing with PBS, the corresponding fluorescent secondary antibody was added and shaken for 2 hours at room temperature, protected from light. Add DAPI staining solution for 20 minutes away from light, and finally observe with a fluorescence-inverted microscope.

2.2.11. Statistical Analysis. The GraphPad Prism software was used for statistical analysis and mapping. Measurement data were expressed as $\overline{x} \pm s$. A one-way analysis of variance was used for the pairwise comparison of multiple samples. $P < 0.05$ indicated that there were significant differences. $P < 0.01$ indicated a significant difference.

3. Results

3.1. Network Pharmacology Analysis

3.1.1. Ingredient-Target Network Analysis. A total of 48 initial chemical components of *P. igniarius* were obtained through TCMSP system retrieval and manual retrieval. According to the standards of the TCMSP and SwissADME systems, the structure of the initial ingredients was verified and screened, and a total of 29 chemical ingredients were flavonoids and compounds of *P. igniarius*. According to the predictions by the SWISS prediction system, seagent, and DisGeNET databases, the ingredient-target network is shown in Figure 2 (Supplementary S1).

3.1.2. Enrichment Analysis. As shown in Figure 3(a), target genes were significantly enriched in cellular response to chemical stress, response to oxidative stress, regulation of cysteine-type endopeptidase activity involved in apoptotic process, and regulation of reactive oxygen species metabolic processes. In addition, endoplasmic reticulum (ER) stress-related pathways involved in the apoptotic process were significantly expressed in the GO enrichment analysis (Supplementary S2). As shown in Figure 3(b), KEGG enrichment analysis indicated that the target genes were significantly involved in the renal cell carcinoma process pathway. Enrichment analysis of TRRUST (Figure 3(c)) in metascape found that these target genes were regulated by many transcription factors, such as HIF1A, ATF4, and so on. Another important point was that many genes were expressed specifically in the kidney. Thus, we established a HUA model by stimulating HK-2 cells with MSU to

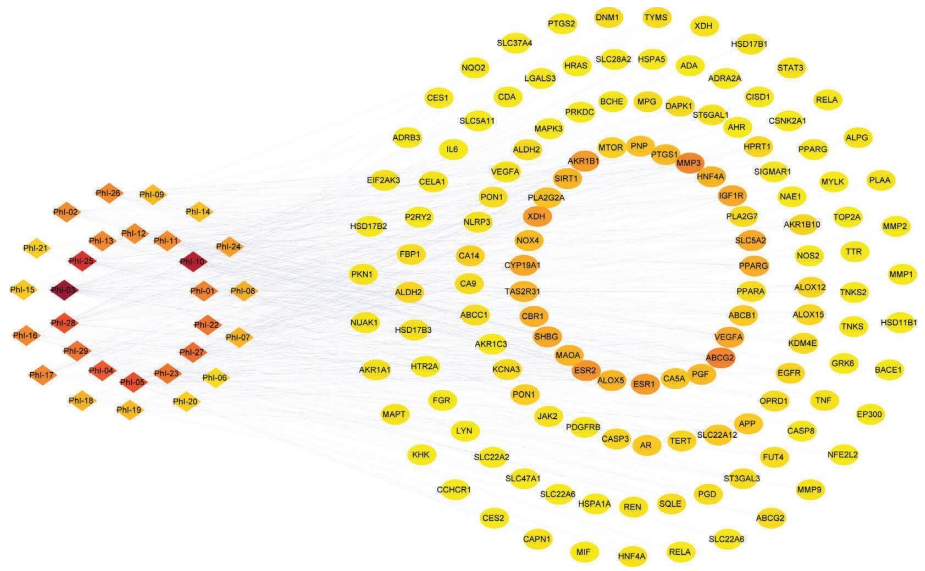

Figure 2: Ingredient-target network of 29 flavonoids from *P. igniarius*.

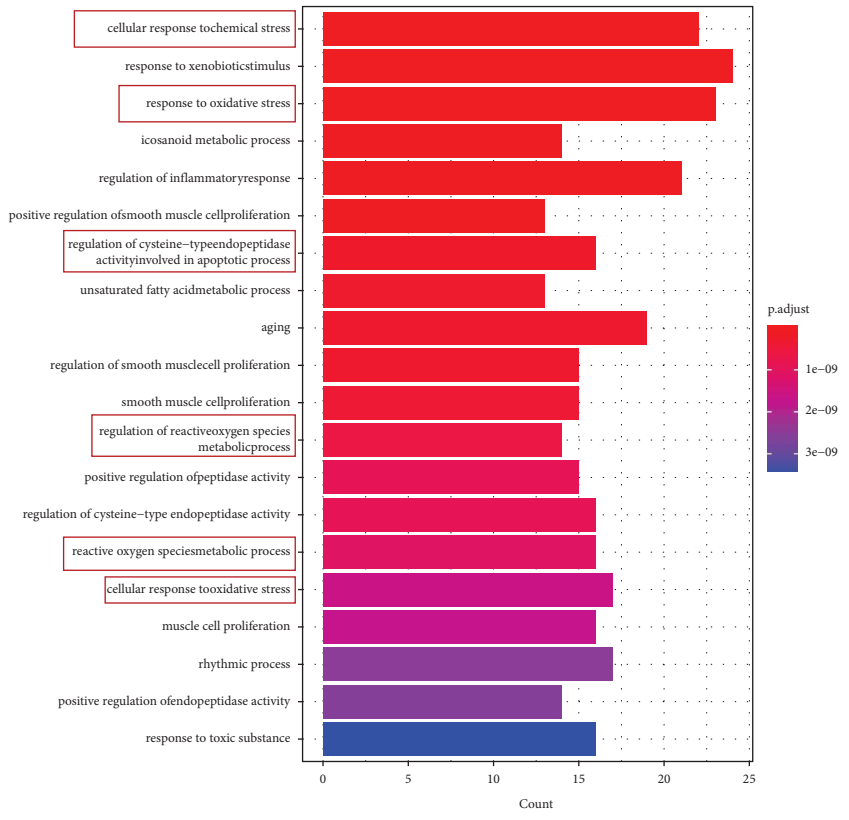

(a)

Figure 3: Continued.

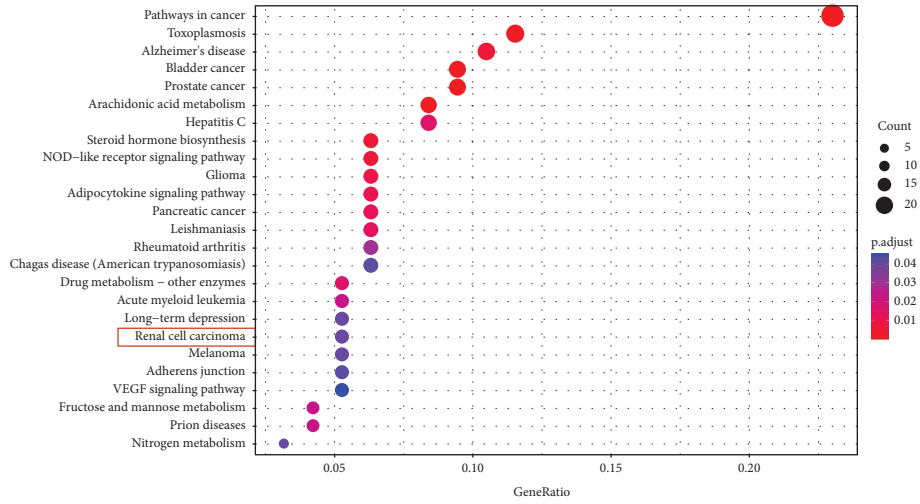

(b)

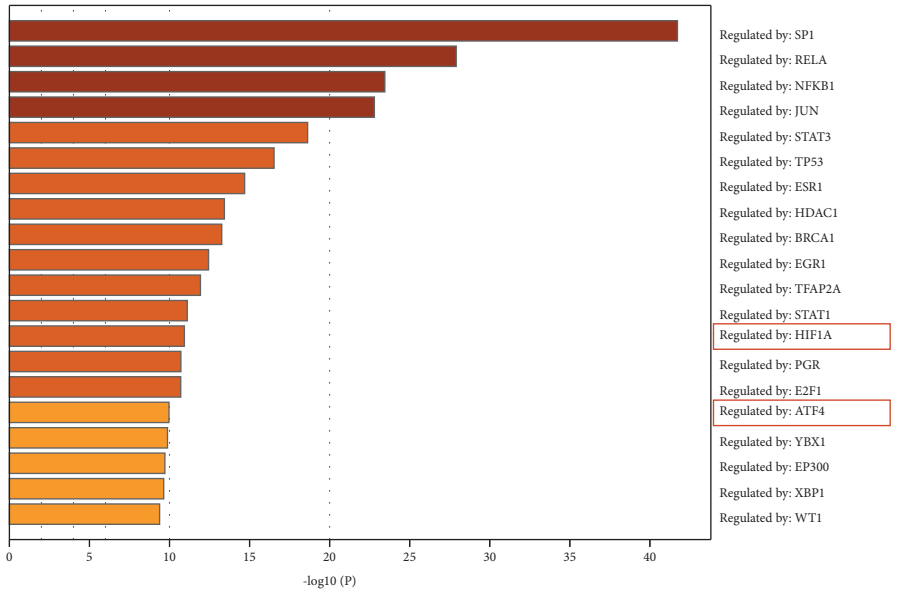

(c)

Figure 3: Network pharmacological enrichment analysis of potential targets. (a) Top 20 terms of GO biological processes. (b) Top 20 terms of KEGG enrichment analysis. (c) Summary of enrichment analysis in TRRUST.

investigate whether total flavonoids from *P. igniarius* could reduce ROS in MSU-induced HK-2 cells, inhibit ER stress, and thereby reduce apoptosis.

3.2. Pharmacodynamic Validation

3.2.1. TFPI Improves the Viability of HK-2 Cells. The preliminary data from our research group showed that 150 μg/mL MSU for 24 h served as the optimal experimental treatment for the cell injury model [14]. TFPI treated with 37.5, 75, and 150 μg/mL for 24 h significantly promoted cell proliferation.

The survival rate of HK-2 cells (Figure 4) was dramatically increased after treatment with different concentrations of TFPI (37.5, 75, and 150 μg/mL) and NAC for 24 h compared to the model group ($P < 0.01$).

3.2.2. TFPI Reduces Oxidative Stress in HK-2 Cells. ROS, SOD, and MDA are all important indicators of oxidative stress response. Compared with the control group, the model group dramatically enhanced the fluorescence intensity (Figures 5(a) and 5(b)), decreased ($P < 0.05$) SOD activity, and increased ($P < 0.01$) MDA content to a significant extent (Figures 5(c) and 5(d)). After treatment, the

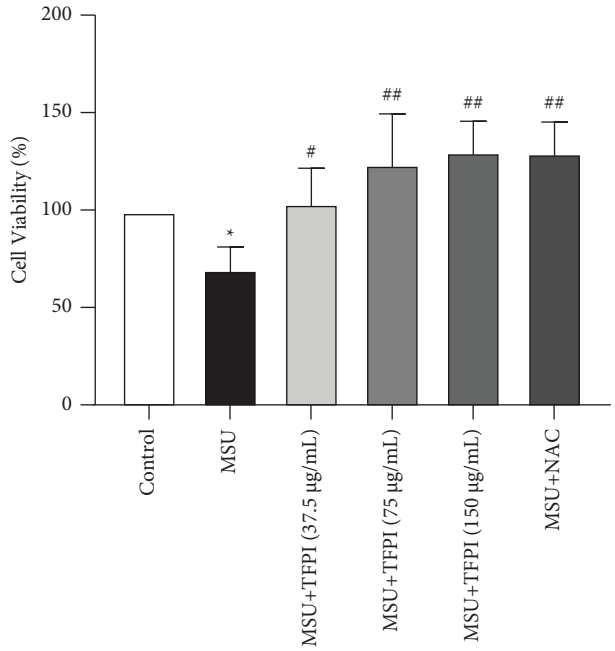

Figure 4: Effect of TFPI on the viability of HK-2 cells by MTT assay. Data are means ± SD ($n = 3$). $^{*}P < 0.05$, as compared to control; $^{\#}P < 0.05$, $^{\#\#}P < 0.01$, as compared to model.

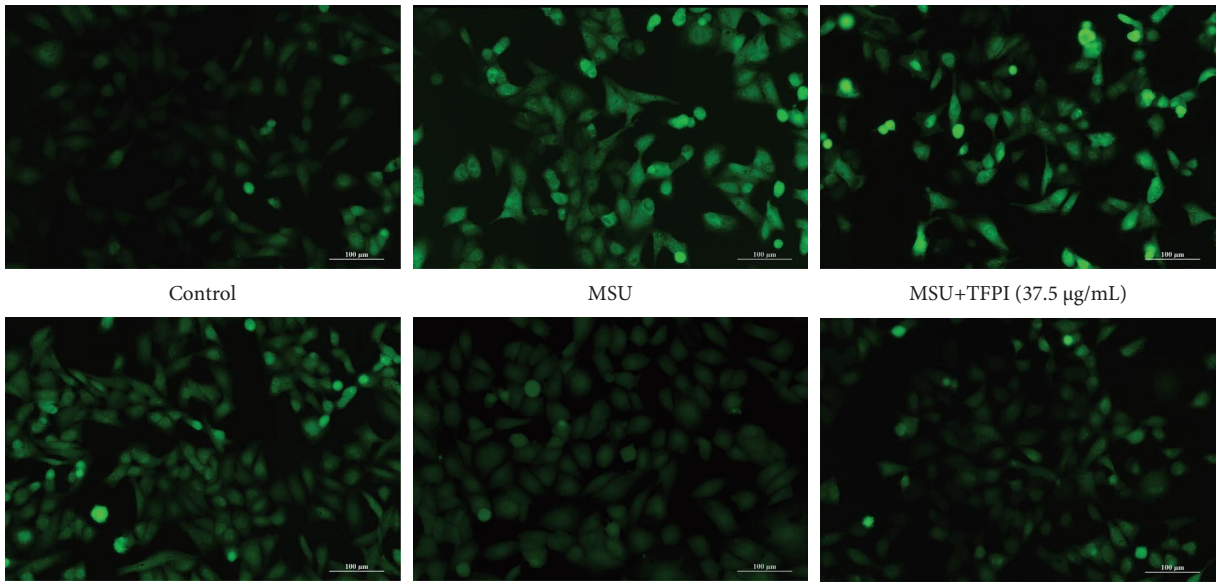

(a)

Figure 5: Continued.

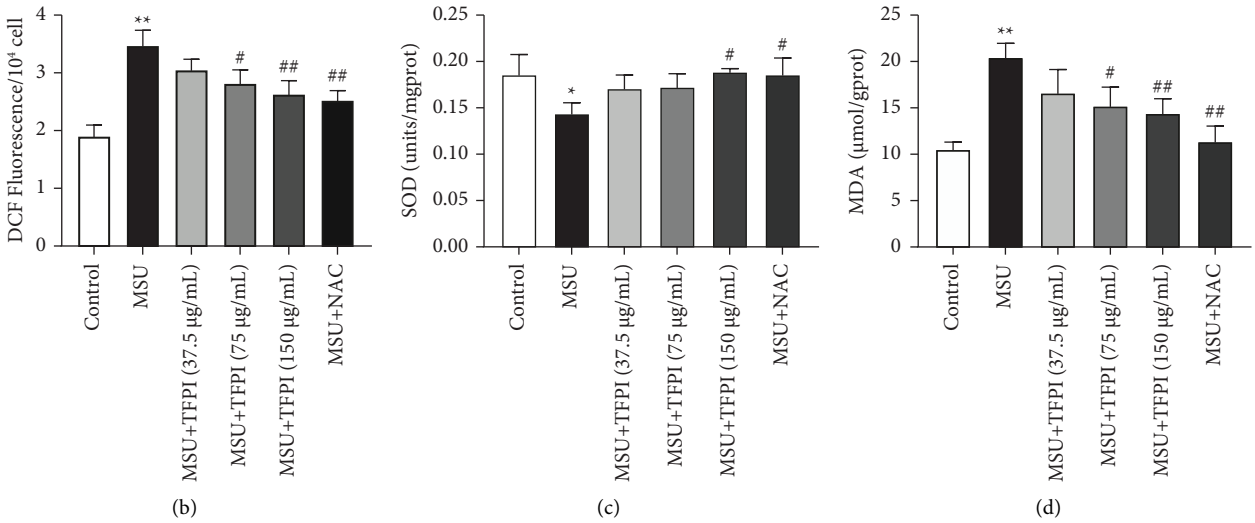

Figure 5: Effect of TFPI on the oxidative stress response of HK-2 cells. (a) Inverted fluorescence microscope observation of fluorescence intensity. (b) ROS fluorescence intensity analysis. (c) Effect of TFPI on SOD activity of HK-2 cells. (d) Effect of TFPI on the MDA content of HK-2 cells. Data are means ± SD ($n = 3$). $^{*}P < 0.05$, $^{**}P < 0.01$, as compared to control; $^{\#}P < 0.05$, $^{\#\#}P < 0.01$, as compared to model.

fluorescence intensity of TFPI treatment groups was decreased in a dose-dependent manner (Figures 5(a) and 5(b)). 150 μg/mL of TFPI and NAC were found to significantly increase ($P < 0.05$) SOD activity (Figure 5(c)), while 75, 150 μg/mL of TFPI and NAC dramatically decreased ($P < 0.05$, $P < 0.01$) MDA content (Figure 5(d)).

The above results indicated that TFPI could significantly suppress the production of ROS and reduce the oxidative stress response in MSU-injured HK-2 cells.

3.2.3. TFPI Increases the Antioxidant Capacity in HK-2 Cells. Figure 6(a) shows that compared with the control group, expression levels of Keap1 were substantially elevated ($P < 0.01$), while the expression levels of Nrf2 and HO-1 were substantially decreased ($P < 0.01$) after induction by MSU. The immunofluorescence experiments (Figure 6(b)) showed that the fluorescence of Nrf2 began to enhance. After TFPI and NAC interventions, the expression trends of the above proteins were antagonized. Red fluorescence was further enhanced in each administration group, indicating an increased transfer of Nrf2 protein from the cytoplasm to the nucleus. This suggested that TFPI could exert antioxidant effects in MSU-injured HK-2 cells through the Keap1/Nrf2 pathway.

3.2.4. TFPI Reduces ROS-Induced Apoptosis in HK-2 Cells. We observed the cell morphology of different treatment groups under an inverted microscope (Figure 7(a)). The number of MSU-induced cells was reduced compared to the control group, and some damaged cells were clearly visible floating in the culture medium. After TFPI and NAC intervention treatment, the number of cells increased with the decrease in floating cells compared to the model group.

To further elucidate the role of TFPI in apoptosis, DAPI staining, LDH assay, and Annexin V-FITC/PI staining were assessed. In MSU-induced HK-2 cells, apoptotic bodies were observed by DAPI staining compared with the control group (Figure 7(b)), while significant increases ($P < 0.01$, $P < 0.01$) were detected in both LDH release rate (Figure 7(c)) and total apoptotic rate (Figure 7(d)). After treatment with TFPI and NAC, the number of apoptotic cells decreased with the increase of TFPI concentration, and the nuclear morphology was close to that of the control group. The LDH release rate and the total apoptosis rate decreased ($P < 0.05$, $P < 0.01$) significantly. All the above results indicated that TFPI had a protective effect on MSU-induced HK-2 cell damage.

3.2.5. TFPI Suppresses ER-Related Protein Expression to Attenuate Apoptosis in HK-2 Cells. ER stress triggers PERK apoptotic signaling pathway mediators, leading to cell injury. We ascertained the impact of TFPI on MSU-induced ER stress response in HK-2 cells via western blot analysis (Figure 8). Compared with the control group, the protein expression levels of Bip, PERK, ATF4, CHOP, BAX, and cleaved caspase 3 were significantly upregulated ($P < 0.01$), and the expression of Bcl-2 protein was significantly downregulated ($P < 0.01$) in the model group. Intervention with TFPI and NAC antagonized this effect by inhibiting ER stress-dependent pathways in a concentration-dependent manner for all proteins compared with the model group.

4. Discussion

With the changes in diet and lifestyle, HUA has become one of the major chronic metabolic diseases in today's society. UA is the end product of purine metabolism and is known to have both antioxidant and pro-oxidant activities [26]. At physiological concentrations, UA (5 mg/dl) is a potent antioxidant, showing antiaging effects on H_2O_2-induced HUVECs and downregulating H_2O_2-induced oxidative stress and inflammation [27]. ROS produced by excessive UA deposition induce cellular oxidative damage [28]. The

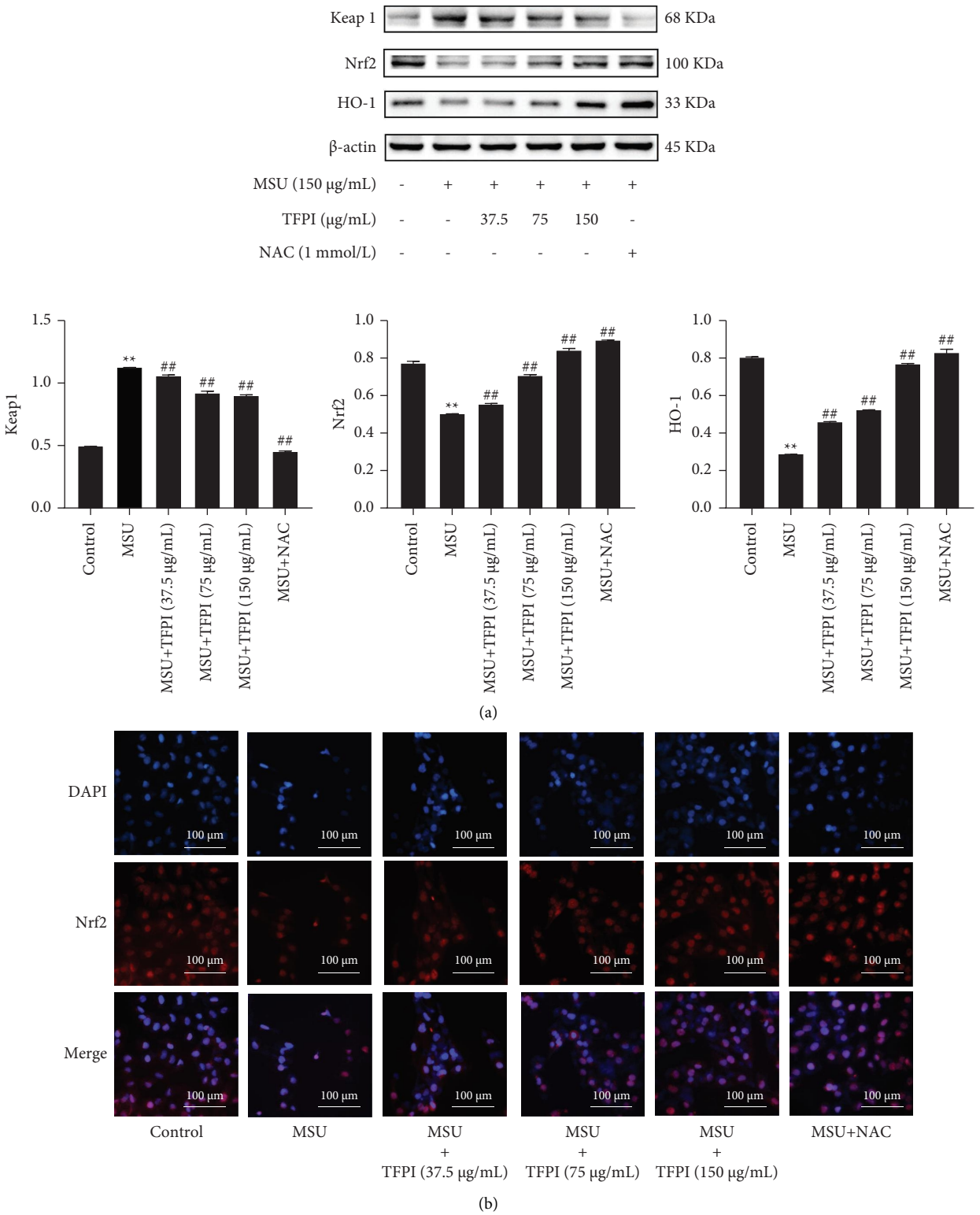

Figure 6: Impact of TFPI on the Keap1/Nrf2 signaling pathway and Nrf2 nuclear displacement in HK-2 cells. (a) Western blot and corresponding histograms of Keap 1, Nrf2, and HO-1 protein expression relative to β-actin. (b) Impact of TFPI on Nrf2 nuclear displacement in HK-2 cells. Data are means ± SD ($n = 3$). $^{**}P < 0.01$, compared with the control; $^{\#\#}P < 0.01$, compared with the model.

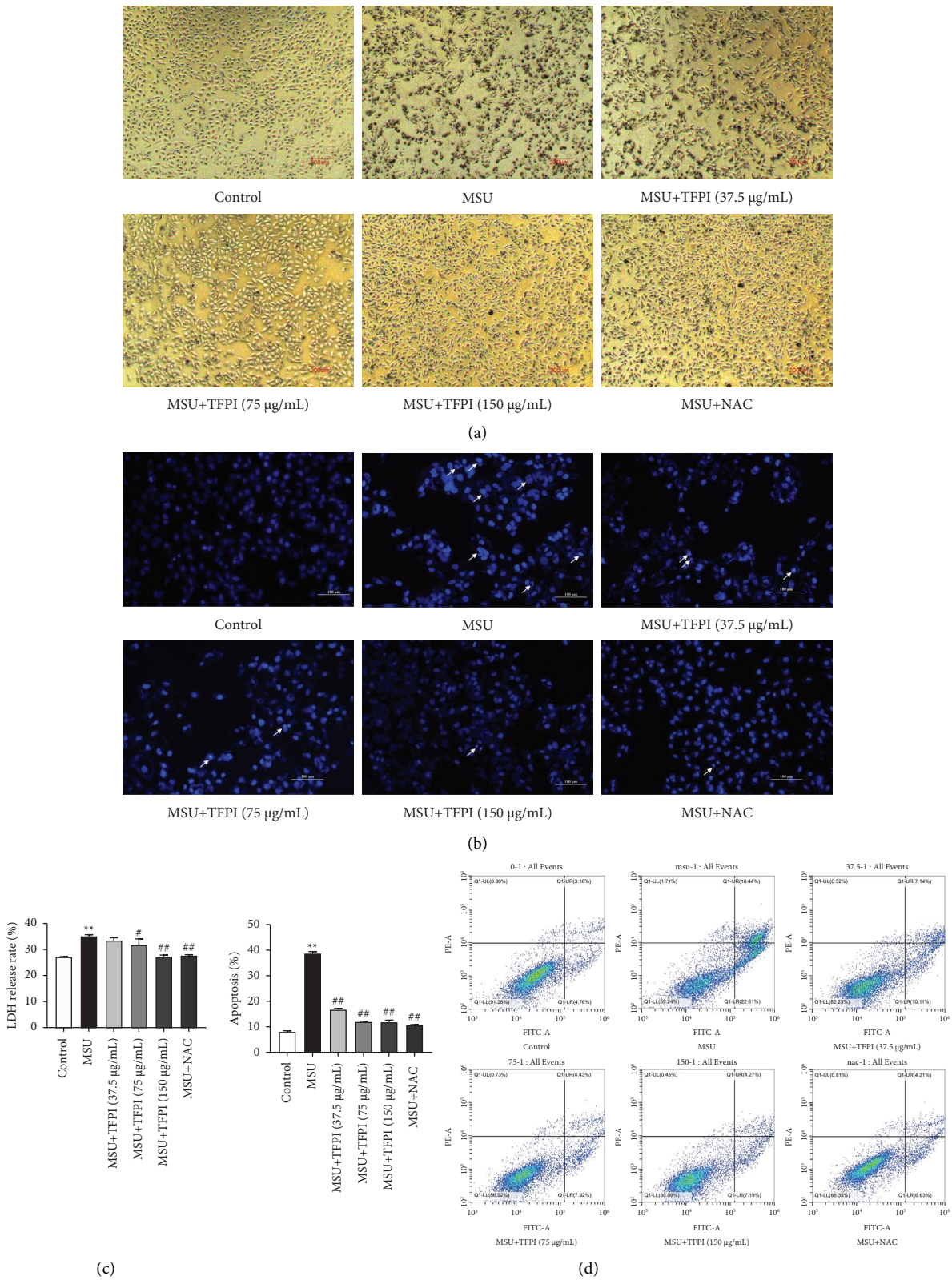

Figure 7: Effect of TFPI on ROS-induced apoptosis in HK-2 cells. (a) Light microscope observation of cell morphology. (b) Fluorescence-inverted microscope observation of cell nuclear morphology. The arrows are to indicate the morphology of nuclear fragmentation. (c) Effect of TFPI on the LDH release rate of HK-2 cells. (d) Flow cytometry was used to detect HK-2 cell apoptosis. Data are means ± SD ($n = 3$). $^{**}P < 0.01$, compared with the control; $^{\#}P < 0.05$, $^{\#\#}P < 0.01$, compared with the model.

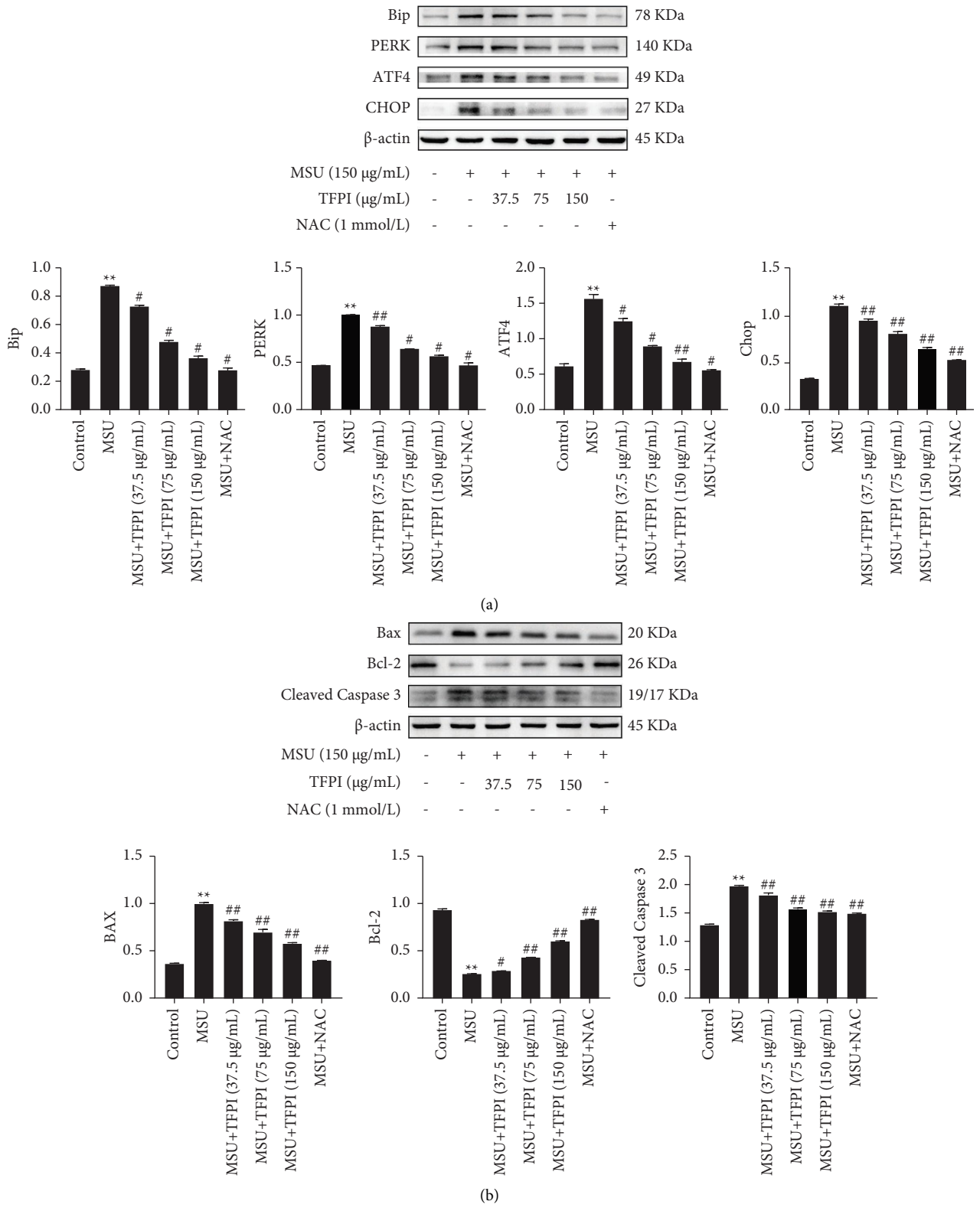

Figure 8: Impact of TFPI on the expression of ER and apoptosis pathway-related proteins in HK-2 cells. (a) Western blot and corresponding histograms of Bip, PERK, ATF4, and chop protein expression relative to β-actin. (b) Western blot and corresponding histograms of BAX, Bcl-2, and cleaved caspase 3 protein expression relative to β-actin. Data are means ± SD ($n = 3$). $^{**}P < 0.01$, compared with the control; $^{\#}P < 0.05$, $^{\#\#}P < 0.01$, compared with the model.

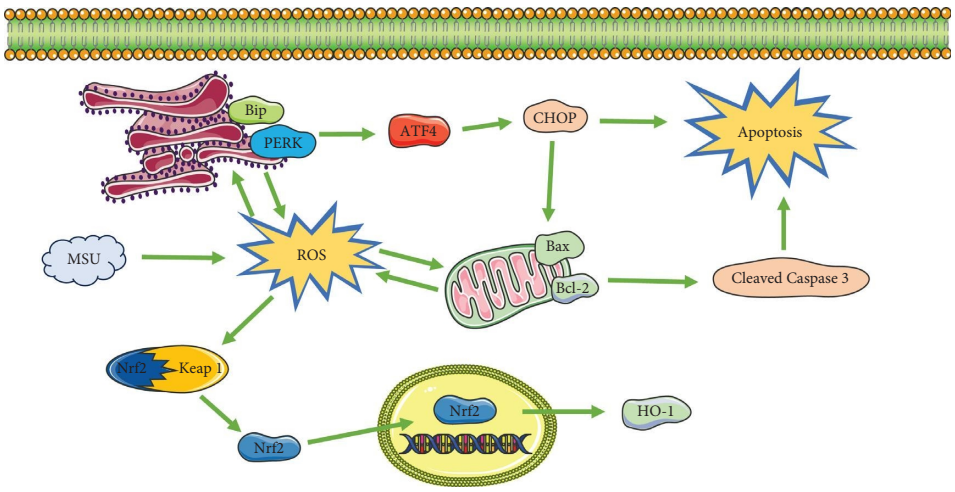

Figure 9: The possible mechanism used by *P. igniarius* to ameliorate HUA.

study found that there was no difference in biochemical parameters except blood UA among asymptomatic young patients with primary HUA; however, the oxidative stress and inflammation in patients were significantly higher than those in healthy people, mainly manifested as increased levels of MDA, SOD, IL-6, and TNF-α, and decreased SOD activity [29].

Network pharmacology prediction results illustrated that TFPI regulated reactive oxygen species metabolism in HUA. The results showed that the intracellular ROS fluorescence intensity was significantly raised in the model group, indicating that MSU stimulated HK-2 cells to cause obvious oxidative damage, and the oxidative stress damage model was successfully established. After treatment with different concentrations of TFPI, the fluorescence intensity of ROS and MDA content in HK-2 cells decreased significantly, while the activity of SOD increased significantly. It was confirmed that TFPI was an effective oxygen radical scavenger and had a significant ameliorating effect on the oxidative stress level of damaged HK-2 cells, but the exact mechanism needs to be further explored.

The Nrf2/HO-1 signaling pathway is one of the classical endogenous antioxidant pathways of the body. When oxidative stress is activated, it activates a series of protective proteins, thereby reducing oxidative stress damage occurring in cells [30–32]. The level of Nrf2 protein expression has an important contribution to HUA, acute kidney injury, chronic kidney disease, nephrotoxicity, and other diseases [33, 34]. Studies have also shown that *Sonneratia apetala* seed oil exerted a urate-lowering effect by restoring the Keap1-Nrf2 pathway, thereby reducing kidney damage caused by HUA [35]. Furthermore, an Nrf2 inhibitor (ML385) also ameliorated HUA-induced insulin resistance [36].

In the normal physiological state of the cell, Nrf2 binds to Keap1 in a heterodimeric manner within the cytoplasm. Upon stimulation by ROS or other electrophile substances, Nrf2 dissociates from Keap1 and transfers to the nucleus. The results showed that Nrf2 and HO-1 protein expression were significantly suppressed in the model group compared with the control group, indicating that the intracellular antioxidant enzyme system was weakened after MSU stimulated HK-2 cells. Then, Nrf2 activates the expression of downstream antioxidant metabolic enzymes (such as HO-1) by binding to the antioxidant response element ARE to reduce oxidative damage and exert a protective effect in cells [37]. When different concentrations of TFPI and NAC were intervened, Keap1 protein expression decreased significantly among the administered groups, while Nrf2 and HO-1 protein expression increased significantly. Interestingly, high concentrations of TFPI (150 μg/mL) had comparable effects with the NAC group. Meanwhile, we also used an IF assay to observe that the intervention of TFPI and NAC not only prompted the transfer of Nrf2 to the nucleus but also produced more Nrf2 in cells to exert antioxidant effects. The results revealed that TFPI had a resistance to MSU-induced oxidative stress damage in HK-2 cells, and we verified that the therapeutic mechanism might be related to a reactivation of the Nrf2/HO-1 signaling pathway, which promoted Nrf2 to enter the nucleus and released HO-1 and other antioxidant substances, thus improving the antioxidant capacity of cells.

ROS also serves as a second messenger to activate multiple signaling pathways to mediate apoptosis [38]. MTT, LDH, and Annexin V-FITC/PI flow cytometry are important means to evaluate cell apoptosis, necrosis and survival status. We found that compared with the control group, the results of Annexin V-FITC/PI flow cytometry in the model group showed a significant increase in the total apoptosis rate, accompanied by important features such as decreased HK-2 cells viability and membrane damage. In addition, apoptotic cells were observed to be smaller in size and produce apoptotic bodies by DAPI staining. After treatment with different concentrations of TFPI and NAC, the survival rate in cells was significantly increased, which further demonstrated the efficacy of TFPI as an oxygen-free

radical scavenger. Then, we investigated the protective mechanism of TFPI against MSU-induced HK-2 cell apoptosis.

Network pharmacology shows that the targets of *P. igniarius* in the treatment of HUA involve the regulation of the apoptotic process, ER stress and the ATF4 transcription factor. Furthermore, studies have shown that ROS-induced chronic ER stress produces a secondary increase in ROS, which usually leads to apoptosis of HK-2 cells [39–41]. ER stress is also closely associated with various renal cell injuries and is involved in mediating the development of renal diseases [42–44]. In the initial stages of ER stress, cells could maintain a stable internal environment through the unfolded protein response (UPR) [45], which is mediated by GRP78 and three stress receptor proteins (ATF6, IRE1, and PERK) [46]. Excessive urate deposition leads to ER stress and disrupts protein folding in the ER [47]. We discussed the effect of TFPI on the expression of PERK signaling pathway-related genes in MSU-induced HK-2 cells. When ER stress occurs, Bip dissociates from PERK, and PERK activation drives phosphorylation of eIF2α, thereby inducing massive ATF4 expression to elicit transcription and expression of downstream CHOP. The elevated level of CHOP expression is a marker of apoptosis initiated by ER stress. CHOP, a proapoptotic protein, also downregulates the expression of Bcl-2 and upregulates the expression of Bax and cleaved caspase 3 protein [48]. We also observed that expression levels of ER-associated proteins (Bip, PERK, ATF4, and CHOP), BAX, and cleaved caspase 3 were dramatically increased in MSU-induced HK-2 cells, while expression levels of Bcl-2 were significantly decreased. TFPI and NAC interventions significantly ameliorated these changes in a concentration-dependent manner following treatment. The above results suggested that ROS is closely associated with ER stress in HK-2 cells, and TFPI inhibited ER stress PERK-ATF4-CHOP pathway activation by reducing ROS to reduce the subsequent induced changes in caspase-dependent apoptosis.

5. Conclusion

Combined with network pharmacology, this study showed that TFPI has a protective effect on MSU-induced oxidative damage in HK-2 cells, and its mechanism may be through activating the Nrf2/HO-1 pathway and inhibiting the ROS-mediated PERK/ATF4/CHOP ER stress pathway to reduce HK-2 cell apoptosis. The possible mechanism used by *P. igniarius* on HUA is shown in Figure 9. These results may provide a novel scientific basis for the development and utilization of *P. igniarius*, as well as for the prevention and treatment of early HUA-associated diseases and kidney disorders resulting from its effects.

Data Availability

The data used to support the findings of this study are available from the corresponding author upon request.

Disclosure

Mengling Lv and Zhouqin Liu share first authorship.

Conflicts of Interest

The authors declare that there are no conflicts of interest regarding the publication of this paper.

Authors' Contributions

ML and ZL conceived and designed the article. ML, ZL, YT, and CJ wrote the paper. ML, ZL, and LH edited the manuscript. All authors read and approved the manuscript. Mengling Lv and Zhouqin Liu contributed equally to this work.

Supplementary Materials

Supplementary Material S1: ingredient-target of 29 flavonoids from *P. igniarius*. Supplementary Material S2: GO enrichment analysis. (*Supplementary Materials*)

References

[1] Z. R. Sun, H. R. Liu, D. Hu et al., "Ellagic Acid Exerts Beneficial Effects on Hyperuricemia by Inhibiting Xanthine Oxidase and NLRP3 Inflammasome Activation," *Journal of Agricultural and Food Chemistry*, vol. 69, no. 43, pp. 12741–12752, 2021.

[2] D. Wu, R. Chen, Q. Li et al., "Tea (camellia sinensis) ameliorates hyperuricemia via uric acid metabolic pathways and gut microbiota," *Nutrients*, vol. 14, no. 13, p. 2666, 2022.

[3] I. Mortada, "Hyperuricemia, type 2 diabetes mellitus, and hypertension: an emerging association," *Current Hypertension Reports*, vol. 19, no. 9, p. 69, 2017.

[4] A. B. Vargas-Santos and T. Neogi, "Management of gout and hyperuricemia in CKD," *American Journal of Kidney Diseases*, vol. 70, no. 3, pp. 422–439, 2017.

[5] F. Marmol, J. Sanchez, and A. Martinez-Pinteno, "Effects of uric acid on oxidative and nitrosative stress and other related parameters in SH-SY5Y human neuroblastoma cells," *Prostaglandins, Leukotrienes and Essential Fatty Acids*, vol. 165, Article ID 102237, 2021.

[6] J. H. Park, Y. I. Jo, and J. H. Lee, "Renal effects of uric acid: hyperuricemia and hypouricemia," *Korean Journal of Internal Medicine (Korean Edition)*, vol. 35, no. 6, pp. 1291–1304, 2020.

[7] C. Yin, B. Liu, Y. Li et al., "IL-33/ST2 induces neutrophil-dependent reactive oxygen species production and mediates gout pain," *Theranostics*, vol. 10, no. 26, pp. 12189–12203, 2020.

[8] M. E. G. Ramirez and J. M. Bargman, "Treatment of asymptomatic hyperuricemia in chronic kidney disease: a new target in an old enemy-a review," *Journal of Advanced Research*, vol. 8, no. 5, pp. 551–554, 2017.

[9] F. Perez-Ruiz, N. Dalbeth, and T. Bardin, "A review of uric acid, crystal deposition disease, and gout," *Advances in Therapy*, vol. 32, no. 1, pp. 31–41, 2015.

[10] X. Wu, S. Wang, C. Liu, C. Zhang, J. Guo, and X. Shang, "A new 2H-benzindazole compound from Alternaria alternata

Shm-1, an endophytic fungus isolated from the fresh wild fruit of *Phellinus igniarius*," *Journal of Natural Medicines*, vol. 73, no. 3, pp. 620–626, 2019.

[11] P. Liu, Y. Xu, J. Ye et al., "Qingre Huazhuo Jiangsuan Decoction promotes autophagy by inhibiting PI3K/AKT/mTOR signaling pathway to relieve acute gouty arthritis," *Journal of Ethnopharmacology*, vol. 302, Article ID 115875, 2023.

[12] H. Zhang, H. Ma, W. Liu et al., "Ultrasound enhanced production and antioxidant activity of polysaccharides from mycelial fermentation of *Phellinus igniarius*," *Carbohydrate Polymers*, vol. 113, pp. 380–387, 2014.

[13] H. Li, X. Zhang, L. Gu et al., "Anti-Gout effects of the medicinal fungus *Phellinus igniarius* in hyperuricaemia and acute gouty arthritis rat models," *Frontiers in Pharmacology*, vol. 12, Article ID 801910, 2021.

[14] D. Chen, C. Jiang, and H. Lu, "Study on the mechanism of *Phellinus igniarius* total flavonoids in reducing uric acid and protecting uric acid renal injury in vitro," *Heliyon*, vol. 9, no. 1, Article ID e12979, 2023.

[15] X. Li, F. J. Chu, S. L. Jiang, and X. B. Jin, "[Preliminary study on effect of *Phellinus igniarius* ethanol extract on serum uric acid metabolism and gut microbiome in rats]," *Zhongguo Zhongyao Zazhi*, vol. 46, no. 1, pp. 177–182, 2021.

[16] L. Shi, Y. Tan, Z. Sun, A. Ren, J. Zhu, and M. Zhao, "Exogenous Salicylic Acid (SA) Promotes the Accumulation of Biomass and Flavonoid Content in *Phellinus igniarius* (Agaricomycetes)," *International Journal of Medicinal Mushrooms*, vol. 21, no. 10, pp. 955–963, 2019.

[17] M. C. Hsin, Y. H. Hsieh, P. H. Wang, J. L. Ko, I. L. Hsin, and S. F. Yang, "Hispolon suppresses metastasis via autophagic degradation of cathepsin S in cervical cancer cells," *Cell Death and Disease*, vol. 8, no. 10, Article ID e3089, 2017.

[18] P. Y. He, Y. H. Hou, Y. Yang, and N. Li, "The anticancer effect of extract of medicinal mushroom Sanghuangprous vaninii against human cervical cancer cell via endoplasmic reticulum stress-mitochondrial apoptotic pathway," *Journal of Ethnopharmacology*, vol. 279, Article ID 114345, 2021.

[19] Y. Sun, S. Zhong, J. Yu et al., "The aqueous extract of *Phellinus igniarius* (SH) ameliorates dextran sodium sulfate-induced colitis in C57BL/6 mice," *PLoS One*, vol. 13, no. 10, Article ID e0205007, 2018.

[20] X. Zhou, Q. Shi, J. Li et al., "Medicinal fungus *Phellinus igniarius* alleviates gout in vitro by modulating TLR4/NF-kB/NLRP3 signaling," *Frontiers in Pharmacology*, vol. 13, Article ID 1011406, 2022.

[21] W. Gao, W. Wang, W. Sun, M. Wang, N. Zhang, and S. Yu, "Antitumor and immunomodulating activities of six *Phellinus igniarius* polysaccharides of different origins," *Experimental and Therapeutic Medicine*, vol. 14, no. 5, pp. 4627–4632, 2017.

[22] Y. Dong, P. Qiu, R. Zhu et al., "A combined phytochemistry and network pharmacology approach to reveal the potential antitumor effective substances and mechanism of *Phellinus igniarius*," *Frontiers in Pharmacology*, vol. 10, p. 266, 2019.

[23] B. Zhu, W. Zhang, Y. Lu et al., "Network pharmacology-based identification of protective mechanism of Panax Notoginseng Saponins on aspirin induced gastrointestinal injury," *Biomedicine and Pharmacotherapy*, vol. 105, pp. 159–166, 2018.

[24] S. He, T. Wang, C. Shi, Z. Wang, and X. Fu, "Network pharmacology-based approach to understand the effect and mechanism of Danshen against anemia," *Journal of Ethnopharmacology*, vol. 282, Article ID 114615, 2022.

[25] Y. Y. Zheng, C. Li, S. L. Feng et al., "[Study on the content determination of total flavonoids in Olea europaea L. leaves]," *Guang Pu Xue Yu Guang Pu Fen Xi*, vol. 31, pp. 547–550, 2011.

[26] Y. Ren, N. Jin, T. Hong et al., "Interactive effect of serum uric acid and total bilirubin for cardiovascular disease in Chinese patients with type 2 diabetes," *Scientific Reports*, vol. 6, no. 1, Article ID 36437, 2016.

[27] Y. Li, L. Zhao, and W. Qi, "Uric acid, as a double-edged sword, affects the activity of epidermal growth factor (EGF) on human umbilical vein endothelial cells by regulating aging process," *Bioengineered*, vol. 13, no. 2, pp. 3877–3895, 2022.

[28] A. Singh, R. Kukreti, L. Saso, and S. Kukreti, "Oxidative stress: a key modulator in neurodegenerative diseases," *Molecules*, vol. 24, 2019.

[29] Y. Zhou, M. Zhao, Z. Pu, G. Xu, and X. Li, "Relationship between oxidative stress and inflammation in hyperuricemia: analysis based on asymptomatic young patients with primary hyperuricemia," *Medicine (Baltimore)*, vol. 97, no. 49, Article ID e13108, 2018.

[30] C. Diao, Z. Chen, T. Qiu et al., "Inhibition of PRMT5 attenuates oxidative stress-induced pyroptosis via activation of the Nrf2/HO-1 signal pathway in a mouse model of renal ischemia-reperfusion injury," *Oxidative Medicine and Cellular Longevity*, vol. 2019, Article ID 2345658, 18 pages, 2019.

[31] J. D. Hayes and A. T. Dinkova-Kostova, "The Nrf2 regulatory network provides an interface between redox and intermediary metabolism," *Trends in Biochemical Sciences*, vol. 39, no. 4, pp. 199–218, 2014.

[32] J. Wang and H. M. Guo, "Astragaloside IV ameliorates high glucose-induced HK-2 cell apoptosis and oxidative stress by regulating the Nrf2/ARE signaling pathway," *Experimental and Therapeutic Medicine*, vol. 17, no. 6, pp. 4409–4416, 2019.

[33] S. Noel, L. J. Arend, S. Bandapalle, S. P. Reddy, and H. Rabb, "Kidney epithelium specific deletion of kelch-like ECH-associated protein 1 (Keap1) causes hydronephrosis in mice," *BMC Nephrology*, vol. 17, p. 110, 2016.

[34] L. M. Shelton, A. Lister, J. Walsh et al., "Integrated transcriptomic and proteomic analyses uncover regulatory roles of Nrf2 in the kidney," *Kidney International*, vol. 88, no. 6, pp. 1261–1273, 2015.

[35] J. Chen, L. Xu, L. Jiang et al., "Sonneratia apetala seed oil attenuates potassium oxonate/hypoxanthine-induced hyperuricemia and renal injury in mice," *Food and Function*, vol. 12, no. 19, pp. 9416–9431, 2021.

[36] W. Yu, C. Chen, W. Zhuang et al., "Silencing TXNIP ameliorates high uric acid-induced insulin resistance via the IRS2/AKT and Nrf2/HO-1 pathways in macrophages," *Free Radical Biology and Medicine*, vol. 178, pp. 42–53, 2022.

[37] Y. Zhang, G. Wang, T. Wang, W. Cao, L. Zhang, and X. Chen, "Nrf2-Keap1 pathway-mediated effects of resveratrol on oxidative stress and apoptosis in hydrogen peroxide-treated rheumatoid arthritis fibroblast-like synoviocytes," *Annals of the New York Academy of Sciences*, vol. 1457, no. 1, pp. 166–178, 2019.

[38] L. J. Su, J. H. Zhang, H. Gomez et al., "Reactive oxygen species-induced lipid peroxidation in apoptosis, autophagy, and ferroptosis," *Oxidative Medicine and Cellular Longevity*, vol. 2019, Article ID 5080843, 13 pages, 2019.

[39] J. D. Malhotra and R. J. Kaufman, "ER stress and its functional link to mitochondria: role in cell survival and death," *Cold Spring Harbor Perspectives in Biology*, vol. 3, no. 9, p. a004424, 2011.

[40] H. Zhang, W. Zhang, F. Jiao et al., "The nephroprotective effect of MS-275 on lipopolysaccharide (LPS)-Induced acute kidney injury by inhibiting reactive oxygen species (ROS)-Oxidative stress and endoplasmic reticulum stress," *Medical Science Monitor*, vol. 24, pp. 2620–2630, 2018.

[41] N. Ye, D. Xie, B. Yang, and M. Li, "The mechanisms of the herbal components of CRSAS on HK-2 cells in a hypoxia/reoxygenation model based on network pharmacology," *Evidence-based Complementary and Alternative Medicine*, vol. 2020, Article ID 5352490, 10 pages, 2020.

[42] A. V. Cybulsky, "Endoplasmic reticulum stress, the unfolded protein response and autophagy in kidney diseases," *Nature Reviews Nephrology*, vol. 13, no. 11, pp. 681–696, 2017.

[43] Y. Fan, W. Xiao, K. Lee et al., "Inhibition of reticulon-1A-mediated endoplasmic reticulum stress in early AKI attenuates renal fibrosis development," *Journal of the American Society of Nephrology*, vol. 28, no. 7, pp. 2007–2021, 2017.

[44] M. Gallazzini and N. Pallet, "Endoplasmic reticulum stress and kidney dysfunction," *Biology of the Cell*, vol. 110, no. 9, pp. 205–216, 2018.

[45] A. E. Frakes and A. Dillin, "The UPR(ER): sensor and coordinator of organismal homeostasis," *Molecular Cell*, vol. 66, no. 6, pp. 761–771, 2017.

[46] R. Iurlaro and C. Munoz-Pinedo, "Cell death induced by endoplasmic reticulum stress," *FEBS Journal*, vol. 283, no. 14, pp. 2640–2652, 2016.

[47] Y. Sun, J. Kang, Z. Tao et al., "Effect of endoplasmic reticulum stress-mediated excessive autophagy on apoptosis and formation of kidney stones," *Life Sciences*, vol. 244, Article ID 117232, 2020.

[48] I. Tabas and D. Ron, "Integrating the mechanisms of apoptosis induced by endoplasmic reticulum stress," *Nature Cell Biology*, vol. 13, no. 3, pp. 184–190, 2011.